# Fundamental Battery Studies
# Final Report

Subcontractor Report
prepared by

*J. B. Goodenough*
*Center for Materials Science and Engineering*
*The University of Texas at Austin*

January 2002

IAT.R 0274

**Approved for public release; distribution unlimited.**

IAT *Institute for Advanced Technology*
*The University of Texas at Austin*

# REPORT DOCUMENTATION PAGE

Form Approved
OMB NO. 0704-0188



| 1. AGENCY USE ONLY (Leave blank) | 2. REPORT DATE | 3. REPORT TYPE AND DATES COVERED |
|---|---|---|
| | January 2002 | technical report, 2001 |

4. TITLE AND SUBTITLE

Fundamental Battery Studies
Final Report

5. FUNDING NUMBERS

Contract # DAAD17-01-D-0001

6. AUTHOR(S)

J. B. Goodenough (Center for Materials Science and Engineering, The University of Texas at Austin)

7. PERFORMING ORGANIZATION NAME(S) AND ADDRESS(ES)

Institute for Advanced Technology
The University of Texas at Austin
3925 W. Braker Lane, Suite 400
Austin, TX 78759-5316

8. PERFORMING ORGANIZATION REPORT NUMBER

IAT.R 0274

9. SPONSORING / MONITORING AGENCY NAME(S) AND ADDRESS(ES)

U.S. Army Research Laboratory
ATTN: AMSRL-WM-B
Aberdeen Proving Ground, MD 21005-5066

10. SPONSORING / MONITORING AGENCY REPORT NUMBER

11. SUPPLEMENTARY NOTES

The view, opinions and/or findings contained in this report are those of the author(s) and should not be considered as an official Department of the Army position, policy, or decision, unless so designated by other documentation.

12a. DISTRIBUTION / AVAILABILITY STATEMENT

Approved for public release; distribution unlimited.

12b. DISTRIBUTION CODE

A

13. ABSTRACT (*Maximum 200 words*)

The objectives of this grant were (1) to analyze the data taken by the Army Research Laboratory (ARL) on the operation of a Saft lithium-ion battery system being developed for pulsed-power applications, (2) to suggest an experimental strategy for determining the relative contributions of electronic and ionic processes in the initial discharge so that a decision could be made either to stop the project or to understand how to optimize performance, and (3) in the absence of feedback from Saft, to pursue an investigation of alternative cathode materials for lithium-ion batteries.

14. SUBJECT TERMS

pulsed power, Saft battery, battery design, lithium-ion battery

15. NUMBER OF PAGES

15

16. PRICE CODE

| 17. SECURITY CLASSIFICATION OF REPORT | 18. SECURITY CLASSIFICATION OF THIS PAGE | 19. SECURITY CLASSIFICATION OF ABSTRACT | 20. LIMITATION OF ABSTRACT |
|---|---|---|---|
| Unclassified | Unclassified | Unclassified | UL |

INTENTIONALLY LEFT BLANK.

## Contents



## List of Figures

INTENTIONALLY LEFT BLANK.

# FUNDAMENTAL BATTERY STUDIES

John B. Goodenough

## INTRODUCTION

The objectives of this grant were (1) to analyze the data taken by the U.S. Army Research Laboratory (ARL) on the operation of a Saft lithium-ion battery system being developed for pulsed-power applications, (2) to suggest an experimental strategy for determining the relative contributions of electronic and ionic processes in the initial discharge so that a decision could be made either to stop the project or to understand how to optimize performance, and (3) in the absence of feedback from Saft, to pursue an investigation of alternative cathode materials for lithium-ion batteries.

## THE PULSED-POWER APPLICATION

The Saft battery developers were attempting to optimize the short-time power delivered through a small-impedance load by a $Li_xC_6//Li_{1-x}CoO_2$ rechargeable battery. In this application, the battery should store both chemical and electrostatic energy. The open-circuit voltage of the battery approaches $V_{OC} \approx 4$ V, and the charge stored is $q = CV_{OC}$, where C is the capacitance of the battery. The charge q may be stored in the bulk of the anode or at the surface of the electrodes and current collectors. The initial current pulse on discharge would contain two components: one due to a capacitance of the current collectors and a rapid desorption of $Li^+$ ions from the anode surface and adsorption from the electrolyte to the cathode surface, and the other due to a slower insertion of $Li^+$ ions from the bulk of the anode to the electrolyte and from the electrolyte into the bulk of the cathode. In the first process, the battery acts as an ultracapacitor, and in the second, as a storage battery. In order to increase the capacitance C of the battery, the Saft developers were making the electrolyte thinner. However, a fundamental question for them was how to determine experimentally the fraction of the discharge current that comes from the faster process relative to the slower process so that they could test the effectiveness of changes in battery design.

## SUGGESTED EXPERIMENTAL STRATEGY

The ARL had developed an equivalent circuit for the battery that allowed tracking of the terminal voltage with time on discharge into a small load impedance. The equivalent circuit contained capacitive and inductive elements, but it provided little insight as to how best to design the battery. We suggested the use of discharge pulses lasting a time $\Delta t$ with a separation between pulses of $\Delta t'$, Fig. 1(a). A rapid drop $-\Delta V$ occurring in the time $\Delta t$ would be followed by a recovery $+\Delta V'$ during $\Delta t'$, Fig. 1(b). The recovery $\Delta V'$ would

be due to bulk ionic processes, and the difference $|\Delta V - \Delta V'|$ would be a measure of the more rapid electronic processes. The Saft developers acknowledged that this was a good strategy, but there was no further feedback as to the results of their experiments.

We further pointed out that the electrodes of ultracapacitors are amorphous, those of batteries are crystalline. Since we are not in the business of optimizing battery fabrication, we left the problem with them and turned to studies of alternative cathode materials for lithium-ion batteries.

## ALTERNATIVE CATHODE MATERIALS

### Manganese Oxospinels

The oxospinel $Li_x[Mn_2]O_4$ has been extensively studied as an alternative to the layered $Li_{1-x}Co_{1-y}Ni_yO_2$ oxides because of cost considerations. In the range $0 < x < 1$, $Li_x[Mn_2]O_4$ gives a voltage $V \approx 4$ V *vs.* a Lithium anode; in the range $1 < x < 2.0$, it gives a $V \approx 3$ V. However, commercial realization has been frustrated by an irreversible capacity fading on cycling in both the 4-V and the 3-V ranges. A flat V *vs.* x curve in the 3-V range signals a wide two-phase domain between a cubic $x = 1.0$ and a tetragonal ($c/a > 1$) $x \approx 1.8$ phase; the Mn(III) concentration in the Li-rich $x \geq 1.8$ phase is high enough to induce a cooperative Jahn-Teller distortion of the spinel to tetragonal ($c/a > 1$) symmetry. The associated change in volume and symmetry tends to break up larger cathode particles on cycling, thus causing a capacity fade. Moreover, $Li[Mn_2]O_4$ in acidic ($pH < 2.0$) aqueous solution induces a surface disproportionation reaction $2Mn(III) = Mn(II) + Mn(IV)$ that is followed by dissolution of $Li^+ + Mn(II)$ to create $\lambda$-$MnO_2 = Li_\delta[Mn_2]O_4$ with $\delta << 1$. Therefore, the possibility that a similar disproportionation reaction may occur in a non-aqueous electrolyte is also a concern. Stabilization of the capacity of the electrode in the 3-V range could involve either the creation of particles of small size or a decoration of the surface with a molecule that would inhibit the surface disproportionation reaction.

In an attempt to decorate the surface of the particles with $Cl^-$ ions, we prepared $Li[Mn_2]O_4$ by a mild sol-gel method in the presence of $MnCl_2 \cdot 4H_2O$. Although we had no $Cl^-$ on the surface of the particles, we found that the capacity of our material was stable over many cycles across the two-phase region at temperatures up to 60°C. Apparently the disproportionation reaction was not a problem on discharge to 2.4 V. However, cycling in the 4-V range still exhibited a capacity fade, but the rate of fading decreased if the cathode was cycled through the 3-V range before returning to the 4-V range. Since some $O_2$ evolution has been observed at the top of the charge, i.e., at V = 4.3 V, we conjecture that octahedral-site Mn(IV) is oxidized to tetrahedral-site Mn(VI) with the loss of $O_2$, and the Mn(VI) that is not lost to the solution may be reduced back to octahedral-site Mn(III) on discharge in the 3-V range.

In order to understand the stability of our cathodes in the 3-V range, we examined our fabrication procedures for $Li[Mn_2]O_4$ prepared by the sol-gel method (SG-LMOS) and by

a conventional solid-state method (SS-LMOS). One step involved ball milling our powders, so we compared the X-ray diffraction (XRD) patterns of hand-ground samples (*e.g.*, SG-LMOSL) with samples that had been ball milled for t minutes (SG-LMOSt or SS-LMOSt). As can be seen in Fig. 2, the XRD peaks were increasingly broadened with ball milling time t. This increase could be due to a reduction in particle size and/or the introduction of lattice strain or stacking faults. The reciprocal-lattice breadths $\beta^*$ of the unmilled powders were almost independent of $\sin\theta$, which indicates negligible lattice strain, whereas the ball-milled spinel powders were found to have a $\beta^*$ strongly dependent on $\sin\theta$ and therefore to contain considerable lattice strain and/or stacking faults. Although the overall particle size was not greatly changed by the ball milling, TEM images and selected-area diffraction (SAD) patterns of the particles, Fig. 3, showed that ball milling created particles with many microdomains.

Thus by a simple step of ball milling the cathode particles for 1h, we have been able to stabilize our $Li_{1+x}[Mn_2]O_4$ ($0 < x < 1$) cathode materials against capacity fade in the 3-V range up to 60°C, as is illustrated by Figs. 4 and 5: the capacity increases with temperature for a given current density because of kinetic considerations. The capacity fade with increasing current density or reduced temperature is reversible.

**$LiNaV_2(PO_4)_3$**

We had previously investigated Lithium insertion into phosphates with the NASICON structure to determine the relative positions of the redox energies of the transition-metal M cations in the $M_2(PO_4)_3$ framework (Appendix A). The V(IV)/V(III) couple was found to give an attractive $V_{OC} = 3.7$ V versus a lithium anode. However, we were not able to prepare $Li_3V_2(PO_4)_3$ in the rhombohedral structure. To obtain the rhombohedral phase, it is necessary to begin with $Na_3V_2(PO_4)_3$ and ion exchange $Li^+$ for $Na^+$. This procedure gave us $Li_2NaV_2(PO_4)_3$. We decided to investigate whether the $Na^+$ ions interfere with the use of this material as a battery cathode. We found we could cycle lithium in and out reversibly; the displacement of some Na to the electrolyte did not cause a problem. The NASICON structure is an open framework that allows rapid diffusion of the $Li^+$ ions. The larger free volume for the $Li^+$ ions reduces the energy density for a standard battery, but if a rapid battery discharge is more important than the energy density, this structure has attractive features.

## ACKNOWLEDGEMENT

The research reported in this document/presentation was performed in connection with Contract number DAAD17-01-D-0001 with the U.S. Army Research Laboratory. The views and conclusions contained in this document/presentation are those of the authors and should not be interpreted as presenting the official policies or position, either expressed or implied, of the U.S. Army Research Laboratory or the U.S. Government unless so designated by other authorized documents. Citation of manufacturer's or trade names does not constitute an official endorsement or approval of the use thereof. The U.S. Government is authorized to reproduce and distribute reprints for Government purposes notwithstanding any copyright notation hereon.

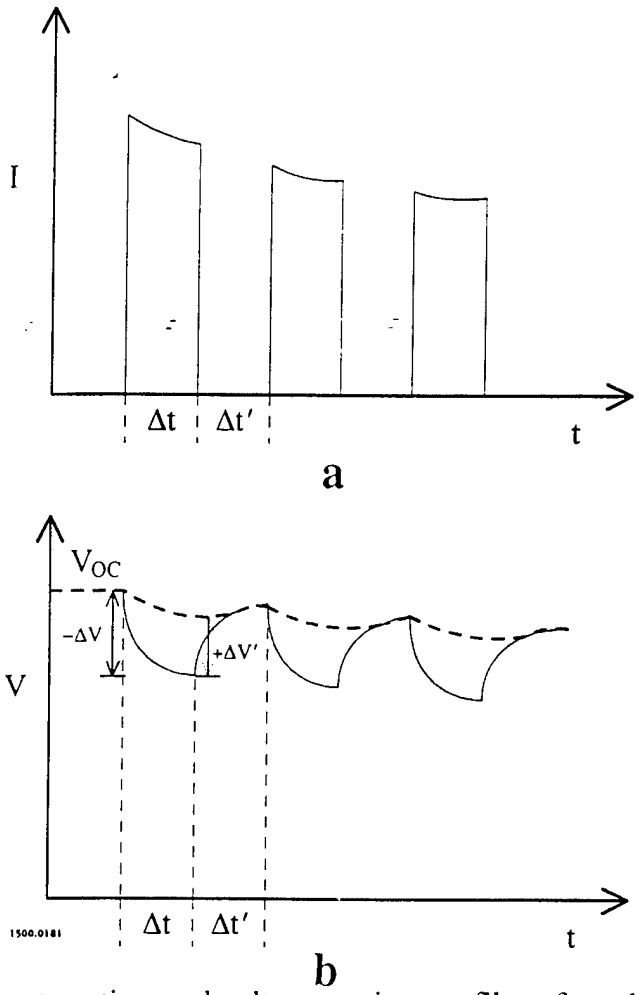


**Figure 1.** Current vs. time and voltage vs. time profiles of a pulsed discharge.

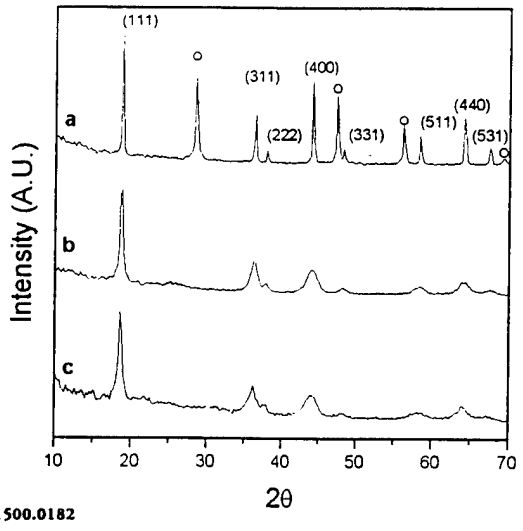


**Figure 2.** XRD patterns. (a) As-prepared, (b) after ballmilling for 60 min., and (c) after ballmilling for 120 min. Open circles denote Si internal standard.

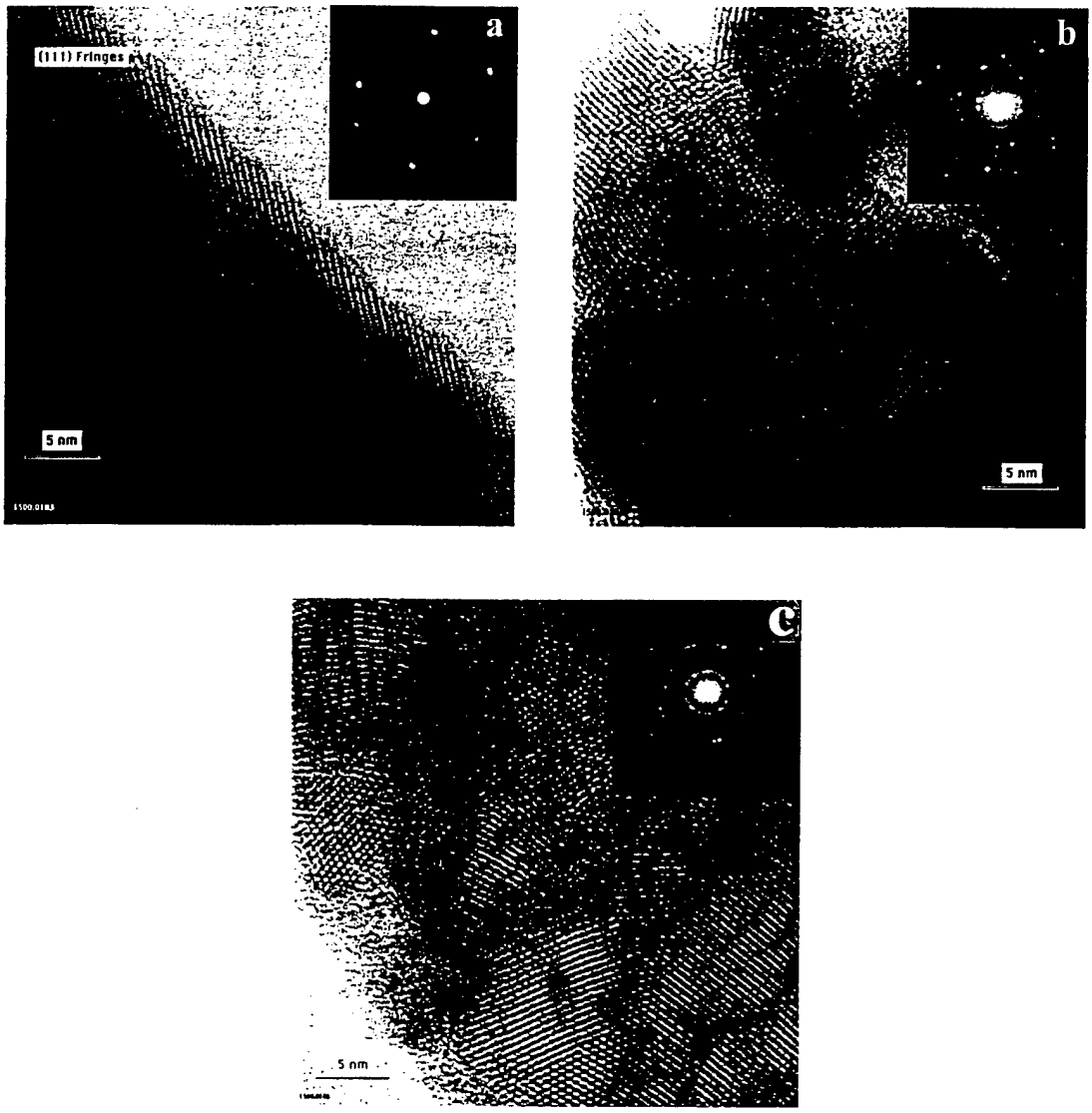


**Figure 3.** TEM images and electron diffraction patterns:
(a) As prepared.
(b) After ballmilling for 60 min.
(c) After ballmilling for 120 min.

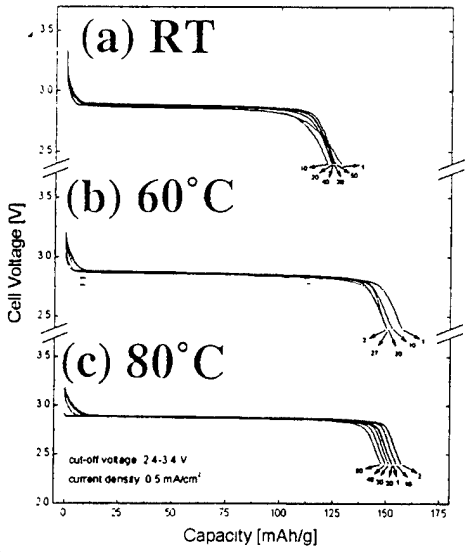


**Figure 4.** Discharge curves of $Li_{1.03}Mn_{1.91}O_4$ ballmilled for 60 min. in the voltage range of 2.4-3.4 at a current density of 0.5 mA/cm$^2$. (a) At room temperature (RT), (b) at 60°C, and (c) at 80°C.

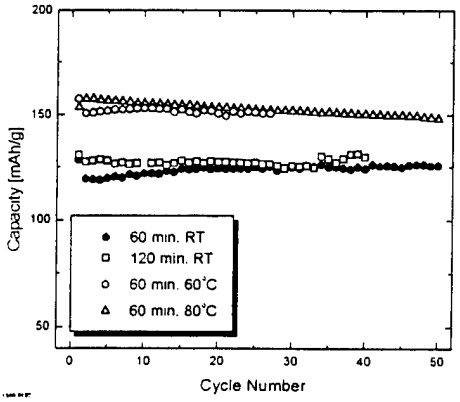


**Figure 5.** Discharge capacities of $Li_{1.03}Mn_{1.91}O_4$ ballmilled for 60 and 120 min. at RT, 60°C, and 80°C.

# Distribution List

Administrator, Defense Technical
Information Center
ATTN: DTIC-DDA
8725 John J. Kingman Road, Suite 944
Ft. Belvoir, VA 22060-6218

Director
U.S. Army Research Lab
ATTN: AMSRL OP SD TA
2800 Powder Mill Road
Adelphi, MD 20783-1145

Director
U.S. Army Research Lab
ATTN: AMSRL OP SD TL
2800 Powder Mill Road
Adelphi, MD 20783-1145

Director
U.S. Army Research Lab
ATTN: AMSRL OP SD TP
2800 Powder Mill Road
Adelphi, MD 20783-1145

Army Research Laboratory
AMSRL-CI-LP
Technical Library 305
Aberdeen Prvg Grd, MD 21005-5066

Dr. Mark Crawford
Institute for Advanced Technology
The University of Texas at Austin
3925 W. Braker Lane, Suite 400
Austin, TX 78759

Dr. Donald Eccleshall
Institute for Advanced Technology
The University of Texas at Austin
3925 W. Braker Lane, Suite 400
Austin, TX 78759

Dr. Harry Fair
Institute for Advanced Technology
The University of Texas at Austin
3925 W. Braker Lane, Suite 400
Austin, TX 78759

Dr. Marilyn Freeman
SAAL-ZT
Suite 9815
2511 Jefferson Davis Highway
Arlington, VA 22202

Charles Hummer
ARL
ATTN: AMSRL-WT-WD
Aberdeen Proving Ground, MD 21005-5066

Mr. Dennis Ladd
Commander, TACOM-ARDEC
Attn: AMSTA-AR-FSP-E / Dennis Ladd
Bldg. 354
Picatinny Arsenal, NJ 07806-5000

Tom Matty
Technology Concepts Management, Inc.
2400 Robbins Station
Irwin, PA 15642

Dr. Ian McNab
Institute for Advanced Technology
The University of Texas at Austin
3925 W. Braker Lane, Suite 400
Austin, TX 78759

Dr. Chadee Persad
Institute for Advanced Technology
The University of Texas at Austin
3925 W. Braker Lane, Suite 400
Austin, TX 78759

# Distribution List

Dr. Jim Sarjeant
State University of New York at Buffalo
312 Bonner-Elect. Engr.
University at Buffalo - SUNY/AB
P. O. Box 601900
Buffalo, NY 14260-1900

Dr. Edward M. Schmidt
U.S. Army Research Laboratory
AMSRL-WM-B
Aberdeen Prvg Grd, MD 21005-5066

Dr. Hardev (Dave) Singh
U.S. Army TACOM-ARDEC
Attn: AMSTA-AR-CCL-D
Building 65N
Picatinny Arsenal, NJ 07806

Jack Taylor
ODUSD
Staff Specialist
1777 North Kent
Suite 9030
Rosslyn, VA 22209

Journal of Solid State Chemistry
doi:10.1006/jssc.2001.9213, available online at http://www.idealibrary.com on IDEAL®

# $Li_2NaV_2(PO_4)_3$: A 3.7 V Lithium-Insertion Cathode with the Rhombohedral NASICON Structure

Brian L. Cushing and John B. Goodenough[1]

*Texas Materials Institute, Mail Code C2201, The University of Texas at Austin, Austin, Texas 78712*

Received February 6, 2001; in revised form April 4, 2001; accepted April 12, 2001

IN HONOR OF PROFESSOR PAUL HAGENMULLER ON THE OCCASION OF HIS 80TH BIRTHDAY

**$Li_2NaV_2(PO_4)_3$ has been prepared in the rhombohedral NASICON structure via ion exchange from $Na_3V_2(PO_4)_3$. As a lithium-insertion cathode material, $Li_2NaV_2(PO_4)_3$ exhibits a specific discharge capacity of $\sim 96\ mAh\ g^{-1}$ at a current density of $0.50\ mA\ cm^{-2}$ with a clear plateau near 3.7 V versus lithium metal. Approximately 10% of the capacity is lost through the first 50 cycles, after which the capacity appears to stabilize. During charge and discharge, the $Na^+$ ions tend to remain immobilized in the $A(1)$ site of the NASICON structure, suggesting a direct $A(2) \rightarrow A(2)$ lithium-transport mechanism.**



*Key Words:* **lithium-insertion compounds; battery; lithium-ion; ion-exchange; mixed alkali–ion conduction.**

## INTRODUCTION

NASICON (for $Na^+$ superionic conductor)-related compounds have been shown to be promising cathode materials for lithium-ion batteries, exhibiting high $Li^+$ mobility and reasonable discharge capacities (1–6). Table 1 details the relevant characteristics of several NASICON-related cathode materials. From Table 1, the transition metals with the most useful redox potentials are $Fe^{2+}/Fe^{3+}$ in a sulfate framework and $V^{3+}/V^{4+}$ in a phosphate framework. $Fe_2(SO_4)_3$ has already been thoroughly investigated as a cathode material for lithium-ion batteries (2,3). Here, we report our investigation of the NASICON-related rhombohedral $Li_2NaV_2(PO_4)_3$ as a high-voltage cathode material.

Cursory examination of the NASICON structure reveals its potential as a lithium-insertion cathode. NASICON-related compounds with the highest ionic mobilities possess rhombohedral ($R\bar{3}$) symmetry (7). The $M_2(XO_4)_3$ framework is built of $(XO_4)^{n-}$ ($X = Si^{4+}, P^{5+}, S^{6+}, Mo^{6+}$, etc.) tetrahedra corner-linked to octahedral-site $M^{m+}$ ($M$ = transition metal) (8). The alkali ions can occupy two different sites. At low alkali content (i.e., $x \leq 1$ in $A_xM_2(XO_4)_3$), an octahedral site, $A(1)$, is selectively occupied (Fig. 1) (8). With $x > 1$, the alkali ions are randomly distributed among the $A(1)$ and three 8-coordinate sites, $A(2)$. The open, 3D nature of the structure allows easy migration of the alkali ions between $A(1)$ and $A(2)$, and the exceptional ionic mobility of the alkali ions is well documented (7).

A NASICON phase, $Li_3V_2(PO_4)_3$, has been previously investigated as a cathode material in lithium batteries (9,10). Like many NASICON-related compounds, however, $Li_3V_2(PO_4)_3$ prepared by direct reaction is not rhombohedral. The $Li_3V_2(PO_4)_3$ phases previously investigated assume the monoclinic ($P2_1/n$) and orthorhombic NASICON structures. The compounds give discharge capacities approaching $131\ mAh\ g^{-1}$, but they also exhibit multiple plateaus in their discharge curves (at 4.1, 3.7, and 3.6 V). Furthermore, previous studies have demonstrated that the monoclinic NASICON modification exhibits reduced alkali-ion mobility relative to the rhombohedral form (6,7). While $Li_3V_2(PO_4)_3$ apparently cannot be prepared in the rhombohedral NASICON structure by direct reaction, rhombohedral $Na_3V_2(PO_4)_3$ has been reported (11) and thus provides a suitable starting material for a topotactic ion exchange of $Li^+$ for $Na^+$.

## EXPERIMENTAL

$Li_2NaV_2(PO_4)_3$ was prepared via ion exchange from $Na_3V_2(PO_4)_3$. $Na_3V_2(PO_4)_3$ was prepared by direct reaction of $NaPO_3$ (prepared by dehydration of $NaH_2PO_4$ (GFS, 99%)) and $V_2O_3$ (Aldrich, 99%) in a 3:1 molar ratio. The reactants were ground under acetone with an agate mortar and pestle. After drying, the mixture was placed in an alumina boat and heated at $1°C\ min^{-1}$ to 900°C under a 10% $H_2$/Ar mixture flowing at $\sim 25\ mL\ min^{-1}$. The sample was held at 900°C for 2 days and slowly cooled to room temperature by turning off the furnace. The product was ground under 5% $H_2SO_4$ to remove any unreacted phosphates, collected by vacuum filtration, and dried at 150°C in air.

[1]To whom correspondence should be addressed.



0022-4596/01 $35.00

**TABLE 1**
**Lithium-Insertion Properties of Selected NASICON-Type Compounds**

| Compound (Ref.) | Structure type[a] | Redox couple | Redox potential (V) | Number of $Li^+$ atoms inserted | Reversible discharge capacity ($mAh\,g^{-1}$)[b] and current ($mA\,cm^{-2}$) |
|---|---|---|---|---|---|
| $Fe_2(SO_4)_3$ (2) | R | $Fe^{3+}/Fe^{2+}$ | 3.6 | 2 | 134 @ 0.015 |
| | M | $Fe^{3+}/Fe^{2+}$ | 3.6 | 2 | 134 @ 0.015 |
| $V_2(SO_4)_3$ (4) | R | $V^{3+}/V^{2+}$ | 2.6 | 1.8 | 130 @ 0.5 |
| $LiTi_2(PO_4)_3$ (5) | R | $Ti^{4+}/Ti^{3+}$ | 2.5 | 2.3 | 160 @ 0.05 |
| | | | | 1.5 | 110 @ 0.5 |
| | | | | 1.2 | 80 @ 1.0 |
| $Li_{3-x}Fe_2(PO_4)_3$ (2, 6) | M | $Fe^{3+}/Fe^{2+}$ | 2.8 | 1.6 | 105 @ 0.05 |
| | | | | 1.1 | 75 @ 0.5 |
| | | | | 0.75 | 55 @ 1.0 |
| $Li_{3-x}FeV(PO_4)_3$ (2) | M | $V^{4+}/V^{3+}$ | 3.8 | 1.6 | 110 @ 0.075 |
| | | $V^{3+}/V^{2+}$ | 1.75 | | |
| | | $Fe^{3+}/Fe^{2+}$ | 2.8 | | |

[a] R = rhombohedral form (space group $R\bar{3}$ or $R\bar{3}c$); M = monoclinic form (space group $P2_1/n$).

[b] Discharge capacity given by $[(nF)/(3.6M_w)]$, $n$ = no. of $Li^+$ atoms inserted per formula unit, $F$ = Faraday's constant (96,485 $C\,mol^{-1}$), $M_w$ = molecular weight of fully intercalated compound.

Ion exchange of $Na_3V_2(PO_4)_3$ was carried out in an aqueous solution containing a 100% molar excess of $LiNO_3$ (GFS, 99.9%) at ~ 40°C. The NASICON phase was stirred in the nitrate solution overnight, collected by vacuum filtration, and washed with deionized water. The process was twice repeated to ensure maximal $Li^+$ for $Na^+$ ion exchange.

Powder X-ray diffraction (XRD) studies were performed on a Philips diffractometer equipped with a Cu$K\alpha$ radiation source ($\lambda$ = 1.5406 Å). Finely divided silicon powder (Aldrich, 99.999%) was used as an internal standard. Peak locations and intensities were determined with the JADE software program using a least-squares method (12).

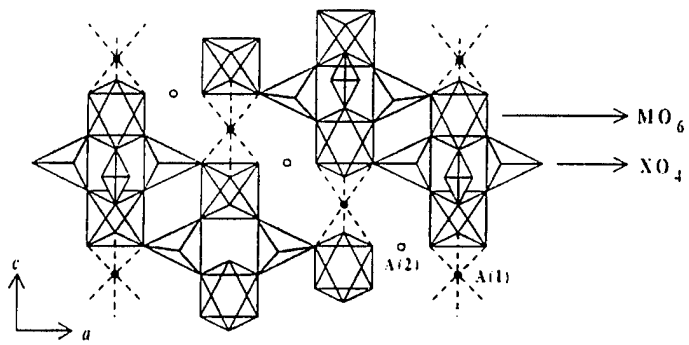


**FIG. 1.** Idealized representation of the rhombohedral form of the NASICON structure.

Quantitative elemental analysis of lithium was carried out on a Perkin-Elmer 1100 Atomic Absorption Spectrometer (AAS). Samples for AAS were digested in concentrated $HNO_3$. Quantitative determinations of vanadium were made by potentiometric titrations. Samples for titration were digested in concentrated $H_2SO_4$. A slight excess of 0.1 M $KMnO_4$ was added to preliminarily oxidize $V^{3+}$ to the pervanadyl ion, $VO_2^+$. The remaining permanganate was reduced by the addition of sodium nitrite, which was subsequently destroyed by the addition of urea. The $VO_2^+$ was then potentiometrically titrated with standard ferrous ammonium sulfate solution. The potentiometric equivalence points were determined by the method of Gran (13).

Electrochemical lithium insertion/extraction was investigated by incorporating $Li_2NaV_2(PO_4)_3$ as cathode materials in lithium-ion button cells (type 2320). The NASICON phase was combined in a 70:25:5 proportion with acetylene black to improve conductivity and polytetrafluoroethylene (PTFE) as a binder. The resulting mixture was rolled into a thin sheet from which 1 $cm^2$ cathode discs of uniform thickness were cut. Cell assembly was carried out in an argon-filled glove box. A 1 M solution of $LiClO_4$ in a 50/50 mixture of propylene carbonate and dimethoxyethane composed the electrolyte. For the button cells, Celgard 2500 served as the separator. The cells were cycled between 2.5 and 4.1 V at 0.50, 1.0, and 2.0 $mA\,cm^{-2}$ against a lithium metal anode on an Arbin BT2043 Battery Test System.

Chemical sodium extraction from $Na_3V_2(PO_4)_3$ was performed by oxidative deintercalation. The NASICON phase was suspended in acetonitrile under inert atmosphere and a 100% molar excess of 1 M $NO_2PF_6$ in acetonitrile was added with standard Schlenk techniques. The mixture was stirred at room temperature for two days under an inert atmosphere. The product was collected by vacuum filtration, washed with acetonitrile, and dried under vacuum.

## RESULTS AND DISCUSSION

$Li_2NaV_2(PO_4)_3$ was obtained via ion exchange of the sodium analogue. Consistent with the findings of others (14), $Na_3V_2(PO_4)_3$ decomposed in molten $LiNO_3$, necessitating that the ion exchange take place in solution at relatively low temperature. During the exchange process, a faint blue coloration of the solution was observed, indicating partial dissolution of the sample. At temperatures above 40°C, the sample dissolution became excessive. Quantitative elemental analysis revealed a final composition of $Li_{1.98}Na_{1.02}V_2(PO_4)_3$, referred to here as $Li_2NaV_2(PO_4)_3$ (Table 2).

Whereas Gopalakrishnan and Kasthuri Rangan (15) reported complete extraction of $Na^+$, we could not oxidatively extract all the $Na^+$ from $Na_3V_2(PO_4)_3$; the composition of our deintercalated product was $Na_{0.99}V_2(PO_4)_3$. This may reflect differences in the experi-

**TABLE 2**
**Elemental Analysis Results for $A_xV_2(PO_4)_3$**

| Compound | % Li [expected] | % Na [expected] | % V [expected] | Experimental composition |
|---|---|---|---|---|
| $Na_3V_2(PO_4)_3$ (starting material) | — | 15.15(4) [15.13] | 22.34(5) [22.35] | $Na_{3.00}V_{2.00}(PO_4)_3$ |
| $Li_2NaV_2(PO_4)_3$ (Exchange product) | 3.24(2) [3.28] | 5.53(3) [5.43] | 24.03(4) [24.05] | $Li_{1.98}Na_{1.02}V_{2.00}(PO_4)_3$ |
| $NaV_2(PO_4)_3$ (Deintercalation product) | — | 5.56(2) [5.61] | 24.88(3) [24.86] | $Na_{0.99}V_{2.00}(PO_4)_3$ |

mental methods, as we used $NO_2PF_6$ as an oxidizing agent as opposed to chlorine gas.

The XRD results for $Li_2NaV_2(PO_4)_3$ indicate that $Li_2NaV_2(PO_4)_3$ retains the rhombohedral NASICON structure of its precursor (Tables 3.4; Fig. 2). The XRD results reveal a substantial contraction of the $a$ parameter and expansion of the $c$ parameter of the rhombohedral NASICON unit cell as $Na^+$ is replaced by $Li^+$. This is consistent with the behavior of other NASICON compounds such as $Na_3Fe_2(PO_4)_3$ during $Li^+$ for $Na^+$ ion exchange (6, 16). Those authors attributed the changes to a redistribution of the alkali ions away from $A(1)$ such that some or all of the $A(1)$ sites are left vacant, which introduces a strong electrostatic repulsion along the $c$ axis across the $A(1)$ site. Delmas *et al.* have demonstrated with neutron diffraction experiments that the exceptional lithium ion conductivity of $Li_{1+x}Ti_2(PO_4)_3$ is due in part to the tendency of $Li^+$ to migrate out of $A(1)$ to $A(2)$ (5). Thus, it would appear that the $Li^+$ cation has a preference for the $A(2)$ site. There is no evidence, however, to indicate a similar behavior for $Na^+$, and in the case of $Li_2NaV_2(PO_4)_3$, $Na^+$ may selectively occupy $A(1)$; otherwise, the $Na^+$ ion should have exchanged for $Li^+$ during the ion-exchange process. $Li^+$ is too small to coordinate at the center of a large, eight-coordinate cavity like $A(2)$; if $Li^+$ is displaced from the center of the cavity, the electrostatic attraction between $Li^+$ and $O^{2-}$ could easily account for the changes in the $c/a$ ratio.

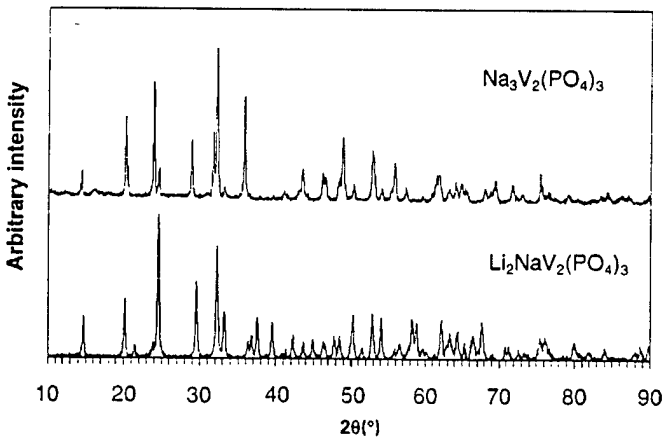


**FIG. 2.** XRD patterns of $Na_3V_2(PO_4)_3$ and $Li_2NaV_2(PO_4)_3$.

*Cathode performance.* The initial charging of the electrochemical cells results in the oxidation of $V^{3+}$ to $V^{4+}$ as 1.8 lithium atoms per formula unit are extracted at $\sim 3.9$ V versus lithium. The subsequent discharge produced a single, flat discharge plateau at 3.7 V (Fig. 3). This value is to be compared with 3.8 V for the $V^{3+}/V^{4+}$ couple found for $Li_{3-x}FeV(PO_4)_3$ (see Table 1). Replacement of one $Li^+$ ion by $Na^+$ has little influence on the energy of the $V^{3+}/V^{4+}$ couple; the dominant influence is the acidity of the polyanion (1–3). At a current density of 0.50 mA cm$^{-2}$, the initial discharge capacity was 96 mAh g$^{-1}$, corresponding to the insertion of 1.5 lithium atoms per formula unit. Consistent with the performance of other NASICON-structured cathodes listed in Table 1, the discharge capacity was diminished by increasing the current density (Fig. 4); the capacity, however, recovered when the current was lowered back to 0.50 mA cm$^{-2}$. This is indicative of a kinetically slow $Li^+$ diffusion process arising from the poor electronic conductivity of the NASICON cathode material. Regardless of

**TABLE 3**
**Summary of Calculated Unit Cells for $A_xV_2(PO_4)_3$**

| Composition | Calculated unit cell | Literature unit cell |
|---|---|---|
| $Na_3V_2(PO_4)_3$ | [Hexagonal]<br>$a = 8.642(9)$ Å<br>$c = 21.72(3)$<br>$V = 1405(5)$ Å$^3$ | [Hexagonal] (11)<br>$a = 8.67(2)$ Å<br>$c = 21.71(3)$<br>$V = 1413(9)$ Å$^3$ |
| $Li_2NaV_2(PO_4)_3$ | [Hexagonal]<br>$a = 8.325(2)$<br>$c = 22.491(6)$<br>$V = 1350(2)$ | This work |

**TABLE 4**
**XRD Results and Indexing for $Li_2NaV_2(PO_4)_3$**

| $h$ | $k$ | $l$ | $d_{obs}$ (Å) | $d_{calc}$ (Å) | $I/I_o$ |
|---|---|---|---|---|---|
| 1 | 0 | 2 | 6.0758 | 6.0695 | 15 |
| 1 | 0 | 4 | 4.4457 | 4.4338 | 32 |
| 1 | 1 | 0 | 4.1611 | 4.1625 | 12 |
| 0 | 0 | 6 | 3.7492 | 3.7485 | 17 |
| 1 | 1 | 3 | 3.6440 | 3.6392 | 100 |
| 2 | 0 | 4 | 3.0350 | 3.0347 | 48 |
| 1 | 1 | 6 | 2.7866 | 2.7855 | 77 |
| 2 | 1 | 1 | 2.7077 | 2.7052 | 33 |
| 2 | 1 | 4 | 2.4519 | 2.4522 | 14 |
| 2 | 0 | 7 | 2.3998 | 2.3986 | 27 |
| 3 | 0 | 3 | 2.2867 | 2.2885 | 25 |
| 1 | 1 | 9 | 2.1437 | 2.1425 | 14 |
| 2 | 1 | 7 | 2.0788 | 2.0782 | 4 |
| 2 | 2 | 1 | 2.0721 | 2.0724 | 4 |
| 3 | 0 | 6 | 2.0232 | 2.0232 | 15 |
| 2 | 1 | 8 | 1.9563 | 1.9570 | 8 |
| 1 | 0 | 10 | 1.9073 | 1.9082 | 6 |
| 3 | 1 | 4 | 1.8822 | 1.8840 | 12 |
| 3 | 0 | 8 | 1.8253 | 1.8268 | 9 |
| 2 | 2 | 6 | 1.8177 | 1.8196 | 22 |
| 4 | 0 | 2 | 1.7809 | 1.7797 | 4 |
| 2 | 1 | 10 | 1.7337 | 1.7346 | 33 |
| 3 | 1 | 7 | 1.6968 | 1.6977 | 23 |
| 3 | 2 | 1 | 1.6472 | 1.6496 | 2 |
| 4 | 0 | 6 | 1.6241 | 1.6244 | 6 |
| 2 | 2 | 9 | 1.6006 | 1.5993 | 8 |
| 3 | 2 | 4 | 1.5873 | 1.5868 | 1 |
| 4 | 0 | 7 | 1.5713 | 1.5720 | 17 |
| 1 | 0 | 14 | 1.5656 | 1.5680 | 2 |
| 4 | 1 | 3 | 1.5404 | 1.5398 | 5 |
| 3 | 1 | 10 | 1.4929 | 1.4944 | 25 |
| 3 | 2 | 7 | 1.4727 | 1.4706 | 1 |
| 2 | 0 | 14 | 1.4668 | 1.4674 | 26 |
| 4 | 1 | 6 | 1.4497 | 1.4507 | 19 |
| 3 | 2 | 8 | 1.4274 | 1.4256 | 5 |
| 1 | 1 | 15 | 1.4113 | 1.4107 | 6 |
| 4 | 0 | 10 | 1.4068 | 1.4065 | 14 |
| 5 | 0 | 4 | 1.3977 | 1.3967 | < 1 |
| 2 | 1 | 14 | 1.3842 | 1.3839 | 32 |
| 2 | 2 | 13 | 1.3302 | 1.3304 | 7 |
| 0 | 0 | 17 | 1.3234 | 1.3230 | 9 |
| 1 | 1 | 17 | 1.2600 | 1.2608 | 18 |
| 3 | 3 | 8 | 1.2440 | 1.2442 | 38 |
| 3 | 1 | 15, 6 0 1 | 1.2000 | 1.1996 | 17 |
| 5 | 1 | 8 | 1.1766 | 1.1761 | 7 |
| 3 | 1 | 16 | 1.1508 | 1.1500 | 8 |
| 4 | 2 | 12 | 1.1008 | 1.1021 | 7 |

current density, capacity fade was evident until about the 50th cycle, at which point the capacities appear to stabilize (Fig. 4).

The presence of $Na^+$ in the cathode material does not lead to cell failure, at least to 100 cycles. Discharge capacity was diminished by about 10% after 50 cycles, but then appeared to stabilize. Previous studies of NASICON cathode materials that contain only $Li^+$ in the $A$ sites, e.g., $Li_3Fe_2(PO_4)_3$, also indicate early capacity fade (2, 6), but to our knowledge, the long-term cycle life of these cathode materials has not been investigated.

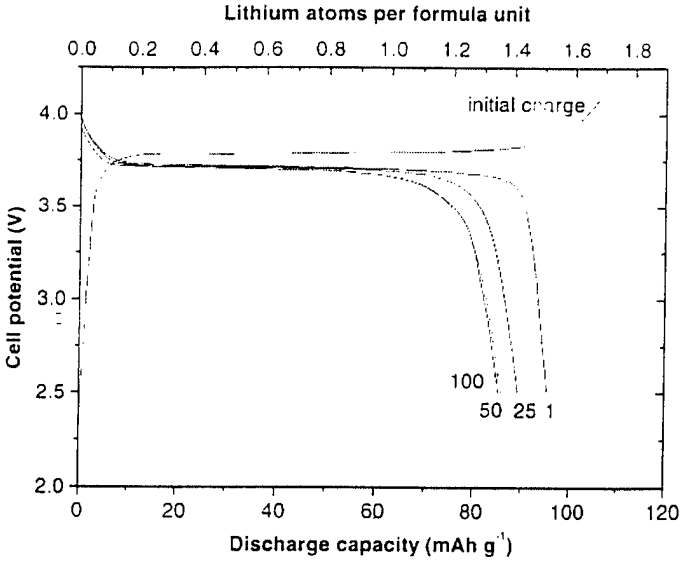


**FIG. 3.** Electrochemical insertion/extraction of rhombohedral $Li_2NaV_2(PO_4)_3$ at a current density of 0.50 mA cm$^{-2}$.

*Ion-transport mechanism.* The ion-exchange behavior of $Na_3V_2(PO_4)_3$ suggests that the two $Na^+$ ions in the $A(2)$ sites are mobile, and thus exchange with $Li^+$, while the $Na^+$ in the $A(1)$ site is not. This result is difficult to reconcile with the established ion-transport mechanism of the rhombohedral NASICON structure, which requires a correlated motion involving both $A(1)$ and $A(2)$ sites:

$$A_1^+(2) + A_2^-(1) + \square(2) \rightarrow \square(2) + A_1^+(1) + A_2^+(2), \quad [1]$$

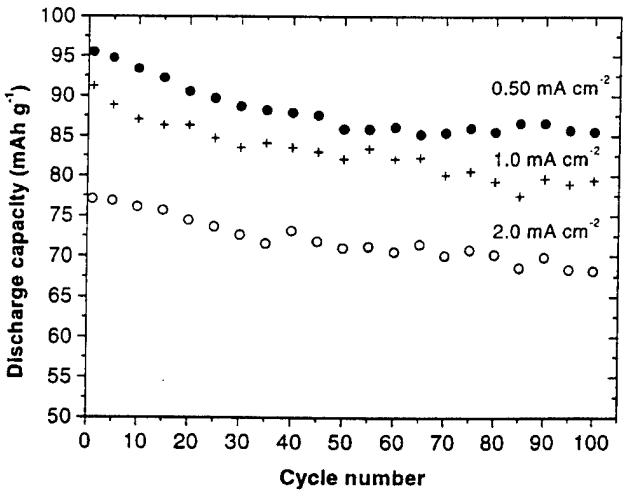


**FIG. 4.** Discharge capacities of rhombohedral $Li_2NaV_2(PO_4)_3$ at various current densities as a function of cycle number.

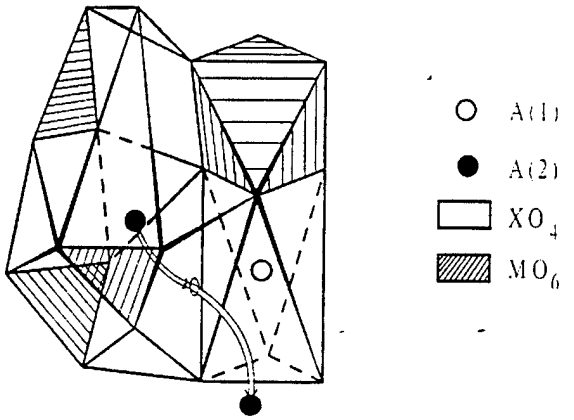


**FIG. 5.** Ion transport pathway between adjacent $A(2)$ sites in the rhombohedral NASICON structure.

where $A$ represents an alkali ion, the number in parentheses denotes the alkali ion in an $A(1)$ or $A(2)$ site, and □ represents a vacancy (7). Thus, if the $Na^+$ ions move in a correlated motion between $A(1)$ and $A(2)$, the ions at both sites should be equally capable of being exchanged for $Li^+$. Likewise, by the mechanism in Eq. [1], both the $Na^+$ ions situated at $A(1)$ and the $Li^+$ ions at $A(2)$ of $Li_2NaV_2(PO_4)_3$ should be capable of being extracted from the structure upon electrochemical charging.

To verify whether the $Na^+$ ions were indeed stationary, the button cells used in the $Li^+$ insertion/extraction experiments were recharged and opened after completion of their 100th cycle and the Na:V ratio in the cathode materials was determined by quantitative elemental analysis. After 100 cycles, 25% of the $Na^+$ ions remained in the cathode material. The $Na^+$ ions that transport out of the NASICON cathode most likely do so while the vanadium is in a mixed III/IV oxidation state, i.e., when $0 < x < 2$ in $Li_xNaV_2(PO_4)_3$. At $x = 0$, only $A(1)$ is occupied and a $Na^+$ ion in that site tends to be immobilized (7). The $x = 2$ condition was realized during the ion-exchange process, yet the $Na^+$ in $A(1)$ clearly did not transport. For the bulk of the time during the charge and discharge processes, the NASICON cathode material exists between the $x = 0$ and $x = 2$ end members, when vanadium is present in varying concentrations of $V^{3+}$ and $V^{4+}$. It seems plausible, then, that the oxidation of vanadium to $V^{4+}$ and the corresponding contraction of its ionic radius introduces a structural distortion to the NASICON framework that reduces the energy difference between $A(1)$ and $A(2)$ and thereby lowers the activation energy of the $A(1) \rightarrow A(2)$ transport pathway.

Notwithstanding the means by which $Na^+$ eventually escapes $A(1)$, the ion-exchange behavior of $Na_3V_2(PO_4)_3$ and the charge/discharge results of $Li_2NaV_2(PO_4)_3$ strongly suggest that Eq. [1] is not the primary ionic transport pathway of this NASICON compound. One possibility is that a direct $A(2) \rightarrow A(2)$ motion is occurring:

$$Li^+(2) + Na^+(1) + \square(2) \rightarrow \square(2) + Na^+(1) + Li^+(2). \quad [2]$$

Interestingly, the possibility of a direct $A(2) \rightarrow A(2)$ conduction pathway has been previously postulated by others (17–21). Whether the $A(2) \rightarrow A(2)$ mechanism is the prevalent conduction in any rhombohedral NASICON compound is a point of contention, but based solely on the geometric considerations of $Li^+$ passing through the opening between adjacent $A(2)$ sites, there is no reason to believe that Eq. [2] is not viable (Fig. 5). Mazza has recently demonstrated with bond-valence calculations that in certain circumstances the $A(2) \rightarrow A(2)$ mechanism can be favored (21). The evidence here suggests that this is precisely the situation in $Li_2NaV_2(PO_4)_3$.

## CONCLUSIONS

The low-temperature ion exchange of $Na_3V_2(PO_4)_3$ resulted in a mixed-alkali NASICON compound, $Li_2NaV_2(PO_4)_3$. As a lithium-insertion cathode, $Li_2NaV_2(PO_4)_3$ produces a discharge capacity of $96\ mAh\ g^{-1}$ at $0.50\ mA\ cm^{-2}$. A 10% capacity fade is evident through the first 50 cycles. The $Na^+$ ions of $Li_2NaV_2(PO_4)_3$ demonstrate a tendency to remain localized in the $A(1)$ site of the rhombohedral NASICON structure. This compound may represent the first empirical evidence of a NASICONcompound in which a direct $A(2) \rightarrow A(2)$ conduction path way is favored over the usual $A(1) \rightarrow A(2) \rightarrow A(1)$ mechanism.

## ACKNOWLEDGMENT

Funding from the Institute for Advanced Technology is gratefully acknowledged.

## REFERENCES

1. A. Manthiram and J. B. Goodenough, *J. Power Sources* **26,** 403 (1989).
2. K. S. Nanjundaswamy, A. K. Padhi, J. B. Goodenough, S. Okada, H. Ohtsuka, H. Arai, and J. Yamaki, *Solid State Ionics* **92,** 1 (1996).
3. A. K. Padhi, V. Manivannan, and J. B. Goodenough, *J. Electrochem. Soc.* **145,** 1518 (1998).
4. J. Gaubicher, J. Angenaut, Y. Chabre, T. Le Mercier, and M. Quarton, *Mol. Cryst. Liq. Cryst.* **311,** 45 (1998).
5. C. Delmas, A. Nadiri, and J. L. Soubeyroux, *Solid State Ionics* **28–30,** 419 (1988).
6. C. Masquelier, A. K. Padhi, K. S. Nanjundaswamy, and J. B. Goodenough, *J. Solid State Chem.* **135,** 228 (1998).
7. J. B. Goodenough, H. Y.-P. Hong, and J. A. Kafalas, *Mater. Res. Bull.* **11,** 203 (1976).
8. H. Y-P. Hong, *Mater. Res. Bull.* **11,** 173 (1976).

9. H. Ohkawa; K. Yoshida, M. Saito, K. Uematsu, K. Toda, and M. Sato, *Chem. Lett.* 1017 (1999).
10. Barker and M. Y. Saidi, U.S. Patent 5, 871, 866,(1999).
11. C. Delmas, R. Olazcuaga, F. Cherkaoui, R. Brochu, and G. Le Flem, *C. R. Acad. Sci. Paris Ser. C* **287,** 169 (1978).
12. JADE, Materials Data Inc., Livermore, CA (2000).
13. G. Gran, *Analyst* **77,** 661 (1952).
14. A. K. Padhi, "Mapping Redox Energies of Electrode Materials for Lithium Batteries," Ph.D. Dissertation, University of Texas at Austin, Austin, Texas, 1997.
15. J. Gopalakrishnan and K. Kasthuri Rangan, *Chem. Mater.* **4,** 745 (1992).
16. C. Masquelier, C. Wurm, J. Rodriguez-Carvajal, J. Gaubicher, and L. Nazar, *Chem. Mater.* **12,** 525 (2000).
17. E. R. Losilla, M. A. G. Aranda, S. Bruque, M. A. Paris, J. Sanz, and A. R. West, *Chem. Mater.* **10,** 665 (1998).
18. D. Tran Qui, J. J. Capponi, M. Gondrand, M. Saïb, J. C. Joubert, and R. D. Shannon, *Solid State Ionics* **3/4,** 219 (1981).
19. M. A. Subramanian, P. R. Rudolf, and A. Clearfield, *J. Solid State Chem.* **60,** 172 (1985).
20. F. Cherkaoui, G. Villeneuve, C. Delmas, and P. Hagenmuller, *J. Solid State Chem.* **65,** 293 (1986).
21. D. Mazza, *J. Solid State Chem.* **156,** 154 (2001).